Published in final edited form as:
Circ Arrhythm Electrophysiol. 2011 June ; 4(3): 388–396. doi:10.1161/CIRCEP.110.959650.

Autonomic Remodeling in the Left Atrium and Pulmonary Veins in Heart Failure – Creation of a Dynamic Substrate for Atrial Fibrillation

Jason Ng, PhD, **Roger Villuendas, MD***, **Ivan Cokic, MD***, **Jorge E. Schliamser, MD, MD**, **David Gordon, MD, PhD**, **Hemanth Koduri, MD**, **Brandon Benefield, MS**, **Julia Simon, BS**, **S. N. Prasanna Murthy, PhD**, **Jon W. Lomasney, MD**, **J. Andrew Wasserstrom, PhD**, **Jeffrey J. Goldberger, MD**, **Gary L. Aistrup, PhD**, and **Rishi Arora, MD**
Feinberg Cardiovascular Rsrch Inst, Northwestern Univ-Feinberg School of Med, Chicago, IL

Abstract

Background—Atrial fibrillation (AF) is commonly associated with congestive heart failure (CHF). The autonomic nervous system is involved in the pathogenesis of both AF and CHF. We examined the role of autonomic remodeling in contributing to AF substrate in CHF.

Methods and Results—Electrophysiological mapping was performed in the pulmonary veins (PVs) and left atrium (LA) in 38 rapid-ventricular paced dogs (CHF group) and 39 controls under the following conditions: vagal stimulation, isoproterenol infusion, β-adrenergic blockade, acetylcholinesterase (AChE) inhibition (physostigmine), parasympathetic blockade, and double autonomic blockade. Explanted atria were examined for nerve density/distribution, muscarinic receptor (MR) and beta-adrenergic receptor (βAR) densities, and AChE activity.

In CHF dogs, there was an increase in nerve bundle size, parasympathetic fibers/bundle, and density of sympathetic fibrils and cardiac ganglia, all preferentially in the posterior LA/PVs. Sympathetic hyperinnervation was accompanied by increases in β_1AR density and in sympathetic effect on ERPs and activation direction. β-adrenergic blockade slowed AF dominant frequency. Parasympathetic remodeling was more complex, resulting in increased AChE activity, unchanged MR density, unchanged parasympathetic effect on activation direction, and decreased effect of vagal stimulation on ERP (restored by AChE inhibition). Parasympathetic blockade markedly decreased AF duration.

Conclusions—In this heart failure model autonomic and electrophysiologic remodeling occurs involving the posterior left atrium and pulmonary veins. Despite synaptic compensation, parasympathetic hyperinnervation contributes significantly to AF maintenance. Parasympathetic and/or sympathetic signaling may be possible therapeutic targets for AF in CHF.

Keywords

atrial fibrillation; autonomic nervous system; heart failure

Correspondence: Rishi Arora, MD, Northwestern University-Feinberg School of Medicine, 251 East Huron, Feinberg 8-503, Chicago, IL 60611, fax: 312-926-2707, phone: 312-695-4954, r-arora@northwestern.edu.
*Drs. Villuendas and Cokic contributed equally as second author

Conflict of Interest Disclosures: None

Atrial fibrillation (AF) is commonly seen in patients with congestive heart failure (CHF).[1] Coexistence of AF and CHF results in increased morbidity and mortality as compared to either condition alone.[2] A variety of structural and electrophysiological changes in the atria contribute to the increased susceptibility to AF in the setting of CHF.[3, 4] Changes in ion-channel expression and gap junction distribution, structural remodeling in the form of fibrosis and oxidative stress are some of the mechanisms that contribute to AF substrate in the setting of CHF.[3–5] In addition, in both clinical and experimental studies, AF has been shown to be mediated at least in part by the autonomic nervous system.[6, 7] It is likely that no single pathophysiological mechanism in and of itself is sufficient to create adequate AF substrate in the CHF setting, with a combination of mechanisms being required to create conditions for the genesis and maintenance of AF. While the role of ion-channel remodeling and fibrosis has been studied extensively in the creation of AF substrate in CHF, the specific contribution of the autonomic nervous system to AF in the setting of CHF has not been well elucidated.

Parasympathetic and sympathetic stimulation have both been demonstrated to be proarrhythmic in the atrium, through refractory period shortening and increased heterogeneity of repolarization.[8] Our previous studies have shown the posterior left atrium (PLA) and pulmonary veins (PVs) have a unique autonomic profile which could help sustain AF in the normal heart.[9] How autonomic effects on atrial electrophysiology are altered by CHF is not completely understood. There is evidence of sympathetic hyperinnervation in patients with AF.[10] While it has recently been suggested that there are increased vagal and sympathetic discharges in CHF that may provide the triggers of AF,[11, 12] the precise nature of autonomic remodeling in AF and its potential role in the creation of AF substrate in CHF have not been studied. We therefore examined in detail structure-function relationships regarding the nature of sympathetic as well as parasympathetic remodeling in the left atrium and PVs during CHF. Our results indicate that autonomic remodeling is not only complex, but is strikingly different in the atrium from what has been reported in the ventricle in the setting of CHF, with the parasympathetic nervous system playing an important role in the creation of AF substrate (unlike in the ventricle, where the vagus appears to be protective against arrhythmias). Sympathetic changes in the CHF atrium also differed from the failing ventricle,[13, 14] with both sympathetic nerves and β-receptors being upregulated in the atrium.

METHODS

Additional methodological details for each of the sections below are described in the Supplemental Material.

Canine CHF Model

Thirty-eight purpose bred hound dogs were used. The details of the pacing model are as previously described.[4, 5] In each dog, sterile surgery for pacemaker implantation was performed. The pacemaker was programmed to pace the right ventricle at a rate of 240 beats per minute. In the first 10 dogs, left ventricular function was assessed during pacing by serial echocardiograms (results for these 10 animals are shown in the Supplemental Material, Figure 1) and clinical symptomology (ascites, tachypnea, reduced physical activity). CHF, indicated by compromised left ventricular function, was confirmed at 3 weeks of pacing. Thirty-nine control dogs (i.e. not paced) were studied for comparison. This protocol conforms to the Guide for the Care and Use of Laboratory Animals published by the U.S. National Institutes of Health (NIH Publication No. 85-23, revised 1996) and was approved by the Animal Care and Use Committee of Northwestern University.

Experimental Setup

Immediately after the 3 weeks of rapid ventricular pacing, a median sternotomy was performed under general anesthesia with isoflurane. High density plaques were applied to the left inferior pulmonary vein (PV; 8 × 5 electrodes; 2.5 mm spacing), the posterior left atrium (PLA; 7 × 3 electrodes, 5 mm spacing) and the left atrial appendage (LAA; 7 × 3 electrodes, 5 mm spacing) for bipolar electrogram recordings and pacing. The PV plaque was placed circumferentially around the vein while the other two plaques were laid flat on the PLA and LAA epicardium. The left cervical vagus nerve was isolated and attached with bipolar electrodes for electrical stimulation.

Autonomic Maneuvers

Effective refractory period (ERP) measurement, activation mapping, and arrhythmia induction (to be described) were performed at baseline and in the presence of the parasympathetic and sympathetic maneuvers described below:

Autonomic blockade

- Complete parasympathetic blockade with atropine (0.04 mg/kg)[15]
- β-adrenergic blockade with propranolol (0.2 mg/kg)[15]
- Double autonomic blockade with propranolol (0.2 mg/kg) and atropine (0.04 mg/kg)

Autonomic stimulation

- Electrical stimulation of the isolated left cervical vagus nerve with a stimulation rate of 20 Hz, pulse width of 5 ms, and amplitude of 10 volts (Grass S44G, Astromed, West Warwick, Rhode Island)
- Acetylcholinesterase (AChE) inhibition through physostigmine infusion IV (3 to 4 mg)
- Combined cervical vagal stimulation in the presence of physostigmine
- Isoproterenol infusion, titrated to increase the sinus rate by 25 percent

In order to exclude M_2R desensitization as a cause of the decrease in vagal-induced ERP shortening, we also assessed for ERP shortening by direct application of carbachol (1mmol/L), a non-selective MR agonist, to the PLA. Upon finishing this *in vivo* portion of the study, the hearts were removed for pathological analysis.

Effective Refractory Periods

To test the autonomic effects on refractoriness, ERPs were obtained from 5, 6, and 4 sites on the PV, PLA, and LAA plaque, respectively, during each autonomic intervention.

Atrial Fibrillation Sustainability and Dominant Frequency

AF induction was attempted in the LAA during baseline, with atropine, and with double autonomic blockade. This protocol consisted of burst pacing at a cycle length of 180 ms to 100 ms (with 10 ms decrements) for 10 seconds at each cycle length. Current was set at four times the threshold for capture. The maximum durations of the AF episodes induced by the burst pacing were calculated for each intervention.

Electrograms recorded during the maximum duration AF episodes obtained by burst pacing were analyzed with dominant frequency (DF) analysis. This analysis was performed offline using Matlab (Mathworks, Natick, MA). Four four-second segments (16 seconds total) of

each channel and AF episode after a stabilization period of four seconds following the cessation of burst pacing were selected for analysis.

Activation Mapping

Recordings from the plaques on the PLA and LAA were made during pacing at a cycle length of 400 ms from the left inferior PV at baseline, parasympathetic blockade, and sympathetic blockade. Activation from the PVs was not analyzed due to insufficient signal quality in the majority of these sites. Creation of activation maps from these recordings and the subsequent analysis were performed offline using custom software programmed in Matlab.

We quantified the similarity of activation patterns between two autonomic conditions by calculating the Pearson's correlation coefficient between two beats, with each beat consisting of activation times obtained by a single multi-electrode plaque. A correlation coefficient of 1 would signify identical activation patterns between a beat at baseline and a beat during autonomic blockade. A correlation coefficient near zero would signify significant change. Correlation coefficients between two repeated beats at baseline and two repeated beats during autonomic blockade were calculated to assess stability of the activation maps. We hypothesized that the similarity in activation patterns between a baseline beat and an autonomic blockade beat would be less than that between two repeated baseline beats. We also hypothesized that the similarity between a baseline beat and an autonomic blockade beat would be different between normal and heart failure dogs. An example of an activation map construction and reproducibility analysis are presented in the Supplemental Material (Figure 2).

Immunohistochemistry

Immunohistochemistry was performed to examine the size and distribution of the parasympathetic (AChE) and sympathetic (dopamine β-hydroxylase, DBH) nerves in the atria. As explained in the expanded Methods section (Supplemental Material), immunostaining was performed on serial sections taken from the PLA, PVs and LAA. Cardiac ganglia were defined as nerve bundles containing one or more neuronal cell bodies. Quantification was performed manually with a light microscope. Mean densities (number per mm^2) of nerve bundles and cardiac ganglia cells were quantified using 1×1 mm grids at 10 times magnification. We also counted the number of parasympathetic and sympathetic fibers within individual nerve bundles. Sizes of nerve bundles were quantified using rectangular 1×1 mm grids at 20 times magnification.

Densities of muscarinic and beta-adrenergic receptors

Radioligand binding assays were used to determine densities of muscarinic and beta-adrenergic receptors (MRs and βARs, respectively) in PV, PLA, and LAA tissue samples. The frozen samples were first powdered and membranes prepared as previously described.[16] The βAR binding assays were performed as described in the Supplemental Material.

AChE activity

The activity of AChE was determined in PV, PLA, and LAA tissue samples. Frozen tissue samples (0.05g) were solubilized and homogenized as described above. Sample supernatants were aliquoted into 96-well microplates and assayed for acetylcholinesterase activity via QuantiChrom™ Acetylcholinesterase Assay kit (Ellman's method) according to the manufacturer's instructions for tissue assay.

Data Analysis

All values are expressed as mean ± standard error. For most analyses, comparisons between CHF and normal dogs were performed with two-way mixed ANOVA with one within-dogs factor (PV vs PLA vs LAA) and one between-dogs factor (CHF vs normal). Student's t tests were used for post-hoc testing. Full factorial mixed effects design with measurement site (PV vs PLA vs LAA) as within-dogs variable and presence of CHF as a between-dogs variable was used to analyze the ERP data separately for each of the study stages (baseline, atropine, propranolol, etc). For the physostigmine analysis, physostigmine was also used as a repeated within-dogs variable. To test the effect of autonomic blockade on the correlation coefficients of activation times, repeated measures ANOVA was used. AF duration between interventions was compared using Student's t test. Statistical significance was taken at p-values less than 0.05.

RESULTS

The breakdown of sample sizes for each intervention/analysis is listed in Table 1. The tissue and molecular assay data are presented first, followed by the *in vivo* electrophysiological data.

Immunohistochemistry

Qualitative observations—Nerve bundles were found to be predominately located in the fibrofatty tissue overlying the epicardium (Figures 1A.i and 1A.ii) in both CHF and normal dogs. Nerve bundles contained either neuronal cells (cardiac ganglia) and/or nerve fibers that arose from the ganglion cells (nerve trunks). Figure 1A.iii shows an example of cardiac ganglia in the PLA; parasympathetic nerve fibers are seen to arise from one of the ganglia (left sided ganglion). Figure 1A.iv shows an example of a ganglion and a nerve trunk side by side. Sympathetic and parasympathetic were found to be co-localized inside the bundles of both the CHF and normal dogs with the amount of parasympathetic fibers dominating over the sympathetic fibers (Figures 1A.i–1A.v).

Quantitative analysis—Figure 1A.v shows an example of a grid over a nerve bundle at 20× magnification. Nerve bundle and nerve fiber density for the PV, PLA, and LAA for the CHF and normal dogs is shown in Figure 1B.i. Nerve bundle density in the PLA was significantly greater than in the PV and LAA. Nerve bundle density was significantly higher in CHF dogs than in normals in the LAA but not in the PV and PLA. Nerve bundle size was significantly larger in the PLA of CHF than of normal dogs (Figure 1B.ii). In addition, the number of parasympathetic fibers/nerve bundle was significantly increased with CHF in the PLA (Figure 1B.iii). The number of sympathetic fibers/nerve bundle did not significantly change with CHF (Figure 1B.iv). Nerve fiber density within nerve bundles was not analyzed in the LAA, due to the very low bundle count in that region. CHF significantly increased the density of cardiac ganglia in the PLA (Figure 1B.v). The number of cell bodies within each ganglion showed a small but non-significant increase (Figure 1B.vi). Sympathetic nerve fiber density was significantly increased in the PV (Figure 1B.vii). There was no significant change in parasympathetic nerve fiber density in either the PV or PLA (Figure 1B.viii).

β-Adrenergic and Muscarinic Acetylcholine Receptor Densities

β_1AR density was increased in the PLA with CHF (Figure 2A), but not in the PV and LAA. There was no change in β_2AR density with CHF in any region (Figure 2B). There was no detected change in MR density with CHF in any region (Figure 2C).

Acetylcholinesterase Activity

Since immunostaining for parasympathetic nerves showed a significant increase in AChE due to an increase in parasympathetic nerve bundle size and ganglion density, we also assessed for AChE activity in the left atrium. As shown in Figure 2D, CHF increased AChE activity in the PV, PLA, and with a trend in the LAA.

Effective Refractory Periods

Baseline—At baseline, the ERPs in CHF dogs were significantly longer than in normal dogs in all regions (Figure 3A).

Autonomic blockade—ERP increase due to propranolol was significantly greater in CHF dogs than in normals in the PV (Figure 3B). ERP increase with atropine was significantly less in CHF compared to normals in the PLA and LAA (Figure 3C). ERP increase with double blockade (atropine and propranolol) was not different between CHF and normals in any region (Figure 3D).

Autonomic stimulation—ERP shortening due to β-adrenergic stimulation with isoproterenol was not significantly different between CHF and normals (Supplemental Material, Figure 3). ERP shortening due to vagal stimulation was significantly less in CHF than in normals in all three regions (Figure 3E). Because immunostaining showed a significant increase in AChE in CHF atria (see Immunohistochemistry section above), and previous data have shown that changes in AChE activity in the synaptic cleft can contribute to vagal desensitization in the heart, we re-assessed vagal effect on ERPs after infusion of physostigmine, an AChE inhibitor. The shortening of CHF ERPs due to vagal stimulation was significantly increased after infusion of physostigmine (Figure 3F), with ERP shortening being equivalent to that noted in normal animals (figure 3E). In contrast, physostigmine infusion did not significantly affect vagal-induced ERP shortening in normal animals (see Supplemental Material, Figure 4). Taken together, the AChE expression/activity data presented in the previous section and the electrophysiology data presented in this section indicate that vagal induced ERP shortening is significantly attenuated in the CHF left atrium due to an increase in AChE activity (in CHF). AChE inhibition restores vagal-induced ERP shortening to normal levels.

In order to exclude M_2R desensitization as a cause of the decrease in vagal-induced ERP shortening, we also assessed for ERP shortening by direct application of carbachol, a non-selective MR agonist, to the PLA. Carbachol application on the CHF PLA also resulted in ERP shortening that was equivalent to that noted in normal dogs (see Supplemental Material, Figure 5).

Atrial Fibrillation Duration

The AF duration results are shown in Figure 4A. The maximum duration of AF episodes induced in these dogs was significantly shorter during parasympathetic blockade with atropine than during baseline. Maximum AF duration with double blockade was also shorter than during baseline. There was no significant effect on AF duration after adding propranolol to atropine than with atropine alone.

Atrial Fibrillation Dominant Frequency

The DF results of the maximum duration AF episodes are shown in Figure 4B. There was no significant difference in mean DF between baseline and with atropine. However, the addition of propranolol to atropine significantly reduced the DF. Figure 4C shows examples of electrograms from the PLA and the corresponding power spectrum and DF for baseline,

atropine, and double blockade. The electrograms with double blockade were slower and more organized in this figure.

Activation mapping

Two paced beats obtained at baseline and two beats obtained in the presence of atropine/propranolol were used to analyze the parasympathetic/sympathetic effect on activation maps in the PLA and LAA of CHF and normal dogs. Reproducibility results are presented in the Supplemental Material.

Correlation coefficients were significantly less when baseline maps were correlated with atropine maps in both normal (Figure 5A.i) and CHF dogs (Figure 5A.ii) compared to the correlation coefficientss from repeated beats. This indicates a significant change in activation with atropine. Propranolol caused a similar change in activation (Figures 5B.i and 5B.ii). The correlation coefficients between baseline and atropine maps were not different in the CHF PLA and LAA than in the normal PLA and LAA (Figure 5A.iii) suggesting that parasympathetic effect on activation is maintained in CHF. However, the correlation coefficients between baseline and propranolol maps were significantly less in both the CHF PLA and LAA than in the normal PLA and LAA (Figure 5B.iii) suggesting an enhanced sympathetic effect on conduction with CHF in both these regions. Figures 5A.iv and 5B.iv show examples of a PLA activation map of a CHF dog during baseline and the altered activation map after atropine and propranolol, respectively.

DISCUSSION

Summary of results

The main findings of this study are that in CHF both parasympathetic and sympathetic remodeling occur in the left atrium, with an increase in both parasympathetic and sympathetic innervation. Notably, neural remodeling was more pronounced in the PLA and PVs than in the rest of the left atrium. Evidence of sympathetic remodeling was an increase in sympathetic nerve fiber density and a concomitant increase in β_1AR. This was accompanied by an increase in sympathetic responsiveness in the PLA and PV, as evidenced by an increase in ERP responsiveness and an enhanced effect on conduction characteristics of these regions. Parasympathetic remodeling was more complex. There was a pronounced increase in parasympathetic innervation, with an increase in nerve bundle size, number of parasympathetic fibers/bundle, cardiac ganglia density, and the number of cell bodies in the ganglia. Vagal hyperinnervation was accompanied by an increase in AChE activity, and a decrease in vagal ERP responsiveness in the left atrium. The increased AChE activity likely represents a compensatory response to vagal hyperinnervation. However, this apparent synaptic compensation was only partial, as parasympathetic contribution to conduction/activation was maintained in the left atrium. Most importantly, parasympathetic blockade led to a significant decrease in AF duration, indicating that parasympathetic activity is an important contributor to AF substrate in CHF. While, double autonomic blockade did not result in a further decrease in AF duration, it did decrease AF dominant frequency, thus indicating the additional influences of sympathetic activity on AF characteristics.

Figure 6 summarizes the results of this study and proposes a working model of how autonomic remodeling in CHF may contribute to the creation of AF substrate.

Dynamic vs. Fixed Substrate for AF

Adequate electrophysiological substrate for AF may be characterized by areas of short refractory periods and slow conduction, and in particular, heterogeneity in repolarization or conduction[5]. In addition to alterations in the ion-channel and gap junction expression that

occur in AF[17], structural abnormalities also contribute to the electrophysiological changes that are necessary for the genesis and maintenance of AF. An important structural abnormality that has been studied extensively for its role in creating electrophysiological abnormalities in the atrium is fibrosis. Fibrosis promotes heterogeneity of conduction and pathways facilitating micro and macrorentry.[5] Our findings suggest that autonomic remodeling may also play a significant role in the creation of AF substrate. It appears that while fibrosis may lead to conduction heterogeneity in the atrium and create a fixed substrate for reentry and consequent AF, parasympathetic and sympathetic remodeling in the PLA and PVs contribute to a more dynamic AF substrate that is dependent on the autonomic state of the left atrium. In fact, even after 3 weeks of rapid ventricular pacing - which typically leads to marked fibrosis in the left atrium[18] - autonomic blockade led to a significant reduction in duration of AF, thereby indicating an important role for the autonomic remodeling in the maintenance of AF. The likely synergism between fibrosis and parasympathetic effect on the creation of AF substrate is as shown in the schematic model proposed in Figure 6.

Relative role of sympathetic vs. parasympathetic remodeling in creating AF substrate in heart failure

Clinical studies suggest that at least in some patients, the sympathetic and/or the parasympathetic nervous system play a role in the genesis of AF[19, 20]. Autonomic fluctuations before the onset of AF have been recognized in several studies. Earlier studies suggested that exercise-induced AF may be sympathetically driven. In contrast, the parasympathetic nervous system may contribute AF in young patients without structural heart disease—i.e., vagal AF.[19] The physiologic studies conducted by Patterson *et al*[21] suggest that adrenergic influences may be playing an important modulatory role in creating adequate substrate for AF, helping provide a necessary ‘catalyst’ for the emergence of focal drivers in the presence of an increased vagal tone.

The results from our study support the notion that the parasympathetic nervous system is the dominant autonomic limb contributing to AF in CHF, with the sympathetic system playing a more modulatory role. Neural remodeling was characterized by increase nerve bundle size and cardiac ganglia density, both of which primarily consist of parasympathetic nerves. Parasympathetic blockade also significantly shortened the duration of AF. A more modulatory role for the sympathetic system is supported by the observation that double autonomic blockade had no addition affect on AF duration, but instead significantly decreased dominant frequency of AF compared to parasympathetic blockade alone.

Our findings clearly highlight the importance of the parasympathetic nervous system in establishing AF substrate in the setting of CHF. However, previous studies have suggested that there is a decrease in parasympathetic tone (which accompanies an increase in sympathetic tone) in CHF, as indicated by a decrease in heart rate variability.[22] It must be remembered however, that heart rate variability is a measure of autonomic modulation on the sinus node, and does not reliably quantify sympathetic and parasympathetic activity.[23] Our study therefore sheds important new light on the autonomic changes induced in this CHF model and their role in genesis of AF.

Differences in parasympathetic and sympathetic remodeling in the atrium versus the ventricle in the setting of heart failure

The sympathetic nervous system appears to promote both atrial and ventricular fibrillation. On the other hand, the parasympathetic nervous system is protective against ventricular fibrillation[24], but is pro-fibrillatory in the atrium, both in normal hearts[25] as well as in CHF (as shown in the current study). This difference is in part due to a differential effect of

parasympathetic stimulation on atrial and ventricular repolarization. Parasympathetic stimulation significantly shortens action potential duration in the atria but either lengthens it[26] or shortens it by a significantly smaller amount in the ventricle[27, 28]. One possible explanation for this difference is the heterogeneity of IK_{Ach} (Kir3.1/3.4) expression in ventricular myocytes, with some ventricular myocytes having little or no IK_{Ach}.[29] In contrast, as we have recently shown, most atrial myocytes – at least in normal hearts - appear to have IK_{Ach} (as demonstrated their sensitivity to acetylcholine and tertiapin Q[16].

Our study also shows that unlike in the failing ventricle[13, 14, 30], where there is a downregulation of β-receptors in the ventricle, there is an upregulation of both sympathetic nerves and β-receptor binding in the CHF atrium (with an accompanying increase in sympathetic responsiveness). The increase in sympathetic innervation we demonstrate in our model is consistent with that previously noted in human AF[31]. Differences in sympathetic remodeling between the atrium and ventricle may be attributed at least in part to CHF being typically more severe in the studies evaluating ventricular autonomic remodeling[13, 14].

Preferential autonomic remodeling in the PLA/PVs: Therapeutic Implications of Current Findings

Our previous work in normal hearts has shown that the PLA and the PVs have a unique autonomic profile compared to other areas of the atrium.[9, 16, 32] Interestingly, in the current study, the greatest changes in autonomic innervation and related autonomic responsiveness in the setting of CHF were also localized to the PVs and PLA, thus underscoring the importance of this region in the genesis and maintenance of AF, especially in the setting of CHF.

These findings have important implications on the treatment of AF in the setting of CHF. Catheter ablation in and around the PV and PLA has recently emerged as a viable therapy for focal AF. However, in patients with structural heart disease e.g. CHF, significantly more extensive ablation has to be performed, in order to increase ‘cure’ rates for AF. Yet, success rates in the setting of structural heart disease do not appear to exceed 50–60%.[33] Our study indicates that the autonomic nervous system contributes to the creation of AF substrate, with the parasympathetic nervous system being involved in the maintenance of AF, and the sympathetic nervous system affecting the frequency characteristics of AF. Targeted approaches to selectively interrupt autonomic signaling in the PLA may therefore help increase the success rates of current ablative or surgical therapies for AF. We have recently shown that inhibition of G_i – the G-protein responsible for downstream parasympathetic signaling in the atrium – by novel $G\alpha_i$ C-terminal inhibitory peptides can allow selective parasympathetic inhibition in the left atrium, with a resulting decrease in vagal induced AF in normal canine hearts[16]. A similar, G-protein targeted approach can potentially be used to selectively inhibit parasympathetic and/or sympathetic signaling in the atrium in the setting of CHF.

Limitations

The time course over which autonomic remodeling occurs was not studied. Thus, it is unknown whether the autonomic remodeling begins shortly after the initiation of pacing or only after structural remodeling has taken place. Furthermore, we did not systematically study the correlation between the echocardiographic/clinical parameters and the extent of autonomic remodeling. The mechanism of burst pacing induced AF may be different from spontaneous clinical AF (spontaneous AF was not observed in this study). As parasympathetic tone is higher in dogs than in humans and the duration of induced CHF is relatively brief, the degree to which these conclusions can be extrapolated to human CHF is as yet undefined. Interpretation of the atrial response to propranolol and atropine may be

complicated by the sympathovagal interactions that occur with autonomic blockade. Autonomic remodeling in the right atrium and in the ventricles was not assessed in this study.

Conclusions

A multifaceted approach was used to demonstrate autonomic remodeling of the atria due to CHF. Further study is necessary to determine whether targeted autonomic blockade in the PLA is capable of inhibiting AF in the setting of CHF.

Supplementary Material

Refer to Web version on PubMed Central for supplementary material.

Acknowledgments

The authors thank Haris Subacius for his statistical contributions, as well as Kathleen Harris, Abigail Angulo, Jacob Goldstein, Laura Davidson, Dr. Anuj Mediratta, and Greg Shade for their assistance with this study.

Funding Sources: NIH [K08HL074192, 1R01HL093490, 3R01HL093490-01S1], Everett/O'Connor Trust.

References

1. Ehrlich JR, Nattel S, Hohnloser SH. Atrial fibrillation and congestive heart failure: specific considerations at the intersection of two common and important cardiac disease sets. J Cardiovasc Electrophysiol. 2002; 13:399–405. [PubMed: 12033360]
2. Wang TJ, Larson MG, Levy D, Vasan RS, Leip EP, Wolf PA, D'Agostino RB, Murabito JM, Kannel WB, Benjamin EJ. Temporal relations of atrial fibrillation and congestive heart failure and their joint influence on mortality: the Framingham Heart Study. Circulation. 2003; 107:2920–2925. [PubMed: 12771006]
3. Everett, THt; Olgin, JE. Atrial fibrosis and the mechanisms of atrial fibrillation. Heart Rhythm. 2007; 4:S24–S27. [PubMed: 17336879]
4. Li D, Melnyk P, Feng J, Wang Z, Petrecca K, Shrier A, Nattel S. Effects of experimental heart failure on atrial cellular and ionic electrophysiology. Circulation. 2000; 101:2631–2638. [PubMed: 10840016]
5. Li D, Fareh S, Leung TK, Nattel S. Promotion of atrial fibrillation by heart failure in dogs: atrial remodeling of a different sort. Circulation. 1999; 100:87–95. [PubMed: 10393686]
6. Chen YJ, Chen SA, Tai CT, Wen ZC, Feng AN, Ding YA, Chang MS. Role of atrial electrophysiology and autonomic nervous system in patients with supraventricular tachycardia and paroxysmal atrial fibrillation. J Am Coll Cardiol. 1998; 32:732–738. [PubMed: 9741520]
7. Zimmermann M, Kalusche D. Fluctuation in autonomic tone is a major determinant of sustained atrial arrhythmias in patients with focal ectopy originating from the pulmunary veins. J Cardiovasc Electrophysiol. 2001; 12:285–291. [PubMed: 11294170]
8. Liu L, Nattel S. Differing sympathetic and vagal effects on atrial fibrillation in dogs: role of refractoriness heterogeneity. Am J Physiol. 1997; 273:H805–H816. [PubMed: 9277498]
9. Arora R, Ng J, Ulphani J, Mylonas I, Subacius H, Shade G, Gordon D, Morris A, He X, Lu Y, Belin R, Goldberger JJ, Kadish AH. Unique autonomic profile of the pulmonary veins and posterior left atrium. J Am Coll Cardiol. 2007; 49:1340–1348. [PubMed: 17394967]
10. Hamabe A, Chang CM, Zhou S, Chou CC, Yi J, Miyauchi Y, Okuyama Y, Fishbein MC, Karagueuzian HS, Chen LS, Chen PS. Induction of atrial fibrillation and nerve sprouting by prolonged left atrial pacing in dogs. Pacing Clin Electrophysiol. 2003; 26:2247–2252. [PubMed: 14675008]
11. Chou CC, Nguyen BL, Tan AY, Chang PC, Lee HL, Lin FC, Yeh SJ, Fishbein MC, Lin SF, Wu D, Wen MS, Chen PS. Intracellular calcium dynamics and acetylcholine-induced triggered activity in

the pulmonary veins of dogs with pacing-induced heart failure. Heart Rhythm. 2008; 5:1170–1177. [PubMed: 18554987]

12. Ogawa M, Zhou S, Tan AY, Song J, Gholmieh G, Fishbein MC, Luo H, Siegel RJ, Karagueuzian HS, Chen LS, Lin SF, Chen PS. Left stellate ganglion and vagal nerve activity and cardiac arrhythmias in ambulatory dogs with pacing-induced congestive heart failure. J Am Coll Cardiol. 2007; 50:335–343. [PubMed: 17659201]
13. Liang C, Rounds NK, Dong E, Stevens SY, Shite J, Qin F. Alterations by norepinephrine of cardiac sympathetic nerve terminal function and myocardial beta-adrenergic receptor sensitivity in the ferret: normalization by antioxidant vitamins. Circulation. 2000; 102:96–103. [PubMed: 10880421]
14. Kawai H, Mohan A, Hagen J, Dong E, Armstrong J, Stevens SY, Liang CS. Alterations in cardiac adrenergic terminal function and beta-adrenoceptor density in pacing-induced heart failure. Am J Physiol Heart Circ Physiol. 2000; 278:H1708–H1716. [PubMed: 10775152]
15. Jose AD, Collison D. The normal range and determinants of the intrinsic heart rate in man. Cardiovasc Res. 1970; 4:160–167. [PubMed: 4192616]
16. Aistrup GL, Villuendas R, Ng J, Gilchrist A, Lynch TW, Gordon D, Cokic I, Mottl S, Zhou R, Dean DA, Wasserstrom JA, Goldberger JJ, Kadish AH, Arora R. Targeted G-protein inhibition as a novel approach to decrease vagal atrial fibrillation by selective parasympathetic attenuation. Cardiovasc Res. 2009; 83:481–492. [PubMed: 19457892]
17. Gollob MH. Cardiac connexins as candidate genes for idiopathic atrial fibrillation. Current opinion in cardiology. 2006; 21:155–158. [PubMed: 16601450]
18. Ohtani K, Yutani C, Nagata S, Koretsune Y, Hori M, Kamada T. High prevalence of atrial fibrosis in patients with dilated cardiomyopathy. J Am Coll Cardiol. 1995; 25:1162–1169. [PubMed: 7897130]
19. Chen PS, Tan AY. Autonomic nerve activity and atrial fibrillation. Heart Rhythm. 2007; 4:S61–S64. [PubMed: 17336887]
20. Chen J, Wasmund SL, Hamdan MH. Back to the future: the role of the autonomic nervous system in atrial fibrillation. Pacing Clin Electrophysiol. 2006; 29:413–421. [PubMed: 16650271]
21. Patterson E, Po SS, Scherlag BJ, Lazzara R. Triggered firing in pulmonary veins initiated by in vitro autonomic nerve stimulation. Heart Rhythm. 2005; 2:624–631. [PubMed: 15922271]
22. Nolan J, Flapan AD, Capewell S, MacDonald TM, Neilson JM, Ewing DJ. Decreased cardiac parasympathetic activity in chronic heart failure and its relation to left ventricular function. Br Heart J. 1992; 67:482–485. [PubMed: 1622699]
23. Piccirillo G, Ogawa M, Song J, Chong VJ, Joung B, Han S, Magrì D, Chen LS, Lin S-F, Chen P-S. Power spectral analysis of heart rate variability and autonomic nervous system activity measured directly in healthy dogs and dogs with tachycardia-induced heart failure. Heart Rhythm. 2009; 6:546–552. [PubMed: 19324318]
24. Ando M, Katare RG, Kakinuma Y, Zhang D, Yamasaki F, Muramoto K, Sato T. Efferent vagal nerve stimulation protects heart against ischemia-induced arrhythmias by preserving connexin43 protein. Circulation. 2005; 112:164–170. [PubMed: 15998674]
25. Tan AY, Chen PS, Chen LS, Fishbein MC. Autonomic nerves in pulmonary veins. Heart Rhythm. 2007; 4:S57–S60. [PubMed: 17336886]
26. Hoffman BF, Suckling EE. Cardiac cellular potentials; effect of vagal stimulation and acetylcholine. Am J Physiol. 1953; 173:312–320. [PubMed: 13065447]
27. Zhang Y, Mazgalev TN. Arrhythmias and vagus nerve stimulation. Heart Fail Rev. 2010
28. Zang WJ, Chen LN, Yu XJ, Fang P, Lu J, Sun Q. Comparison of effects of acetylcholine on electromechanical characteristics in guinea-pig atrium and ventricle. Exp Physiol. 2005; 90:123–130. [PubMed: 15466461]
29. Dobrzynski H, Marples DD, Musa H, Yamanushi TT, Henderson Z, Takagishi Y, Honjo H, Kodama I, Boyett MR. Distribution of the muscarinic K+ channel proteins Kir3.1 and Kir3.4 in the ventricle, atrium, and sinoatrial node of heart. J Histochem Cytochem. 2001; 49:1221–1234. [PubMed: 11561006]

30. Kawai H, Fan TH, Dong E, Siddiqui RA, Yatani A, Stevens SY, Liang CS. ACE inhibition improves cardiac NE uptake and attenuates sympathetic nerve terminal abnormalities in heart failure. Am J Physiol. 1999; 277:H1609–H1617. [PubMed: 10516201]

31. Gould PA, Yii M, McLean C, Finch S, Marshall T, Lambert GW, Kaye DM. Evidence for increased atrial sympathetic innervation in persistent human atrial fibrillation. Pacing Clin Electrophysiol. 2006; 29:821–829. [PubMed: 16922997]

32. Arora R, Ulphani JS, Villuendas R, Ng J, Harvey L, Thordson S, Inderyas F, Lu Y, Gordon D, Denes P, Greene R, Crawford S, Decker R, Morris A, Goldberger J, Kadish AH. Neural substrate for atrial fibrillation: implications for targeted parasympathetic blockade in the posterior left atrium. Am J Physiol Heart Circ Physiol. 2008; 294:H134–H144. [PubMed: 17982017]

33. Wright M, Haissaguerre M, Knecht S, Matsuo S, O'Neill MD, Nault I, Lellouche N, Hocini M, Sacher F, Jais P. State of the art: catheter ablation of atrial fibrillation. J Cardiovasc Electrophysiol. 2008; 19:583–592. [PubMed: 18462322]

Atrial fibrillation (AF) is common in patients with heart failure. While atrial fibrosis is a likely factor, other factors are also likely important. This study suggests that the autonomic nervous system also contributes significantly to the formation of AF substrate in a canine model of heart failure. We found that unlike the failing ventricle, where there appears to be parasympathetic withdrawal, there is an increase in parasympathetic innervation in the failing atrium, which appears to contribute to the maintenance of AF. We also show that both sympathetic and parasympathetic remodeling occur and are most pronounced in the posterior left atrium (PLA). These findings support further evaluation of ablation of autonomic ganglionated plexi to improve the success AF ablation in heart failure. The data also support exploration of the parasympathetic nervous system as a therapeutic target for prevention of AF in the failing heart.

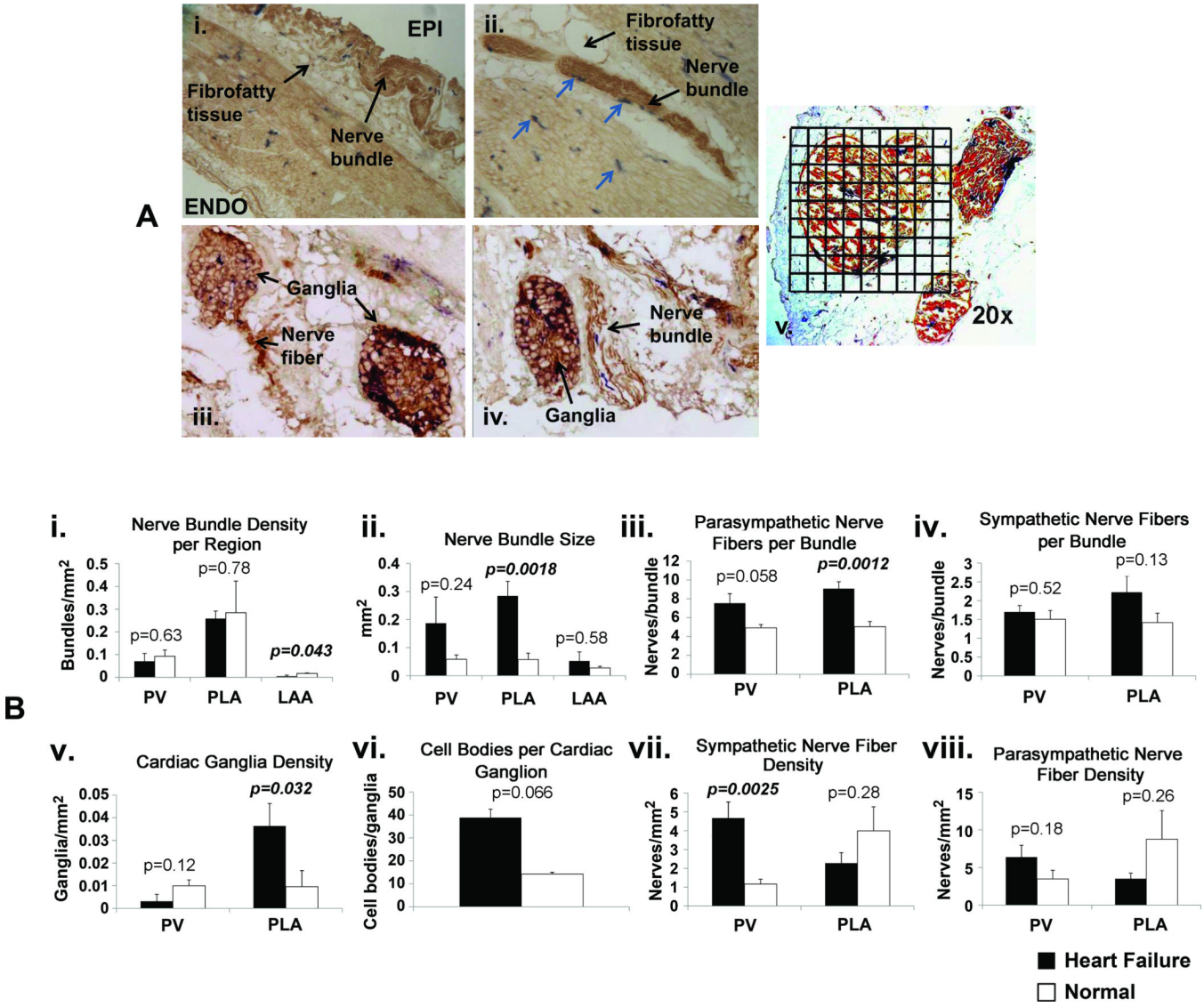

Figure 1.

Panel A: Examples of sympathetic and parasympathetic nerve staining. A.i. – example of a nerve bundle located in the fibrofatty tissue overlying the epicardium (EPI) (10×). ENDO – endocardium. A.ii. – example of nerve bundles located in fibrofatty tissue on the epicardial aspect of PV (4×). Sympathetic fibers are in blue (arrows). A.iii. – examples of cardiac ganglia, with parasympathetic fibers arising from cardiac ganglion on the left side (20×). A.iv. - example of cardiac ganglia on the left and nerve bundle on the right; nerve fibers showing co-localized sympathetic (blue) and parasympathetic fibers (brown) (20×). A.v. - illustration of the use of 1 mm × 1 mm grids to quantify the cross-sectional area of a nerve bundle at 20× magnification. Panel B: Quantitative analysis of nerve staining. B.i. – nerve bundle density, B.ii. – nerve bundle size, B.iii. – number of parasympathetic nerve fibers/ bundle, B.iv. – number of sympathetic nerve fibers/bundle, B.v. – density of cardiac ganglia, B.vi. – number of cell bodies/cardiac ganglion, B.vii - density of sympathetic fibers, B.viii. – density of parasympathetic fibers.

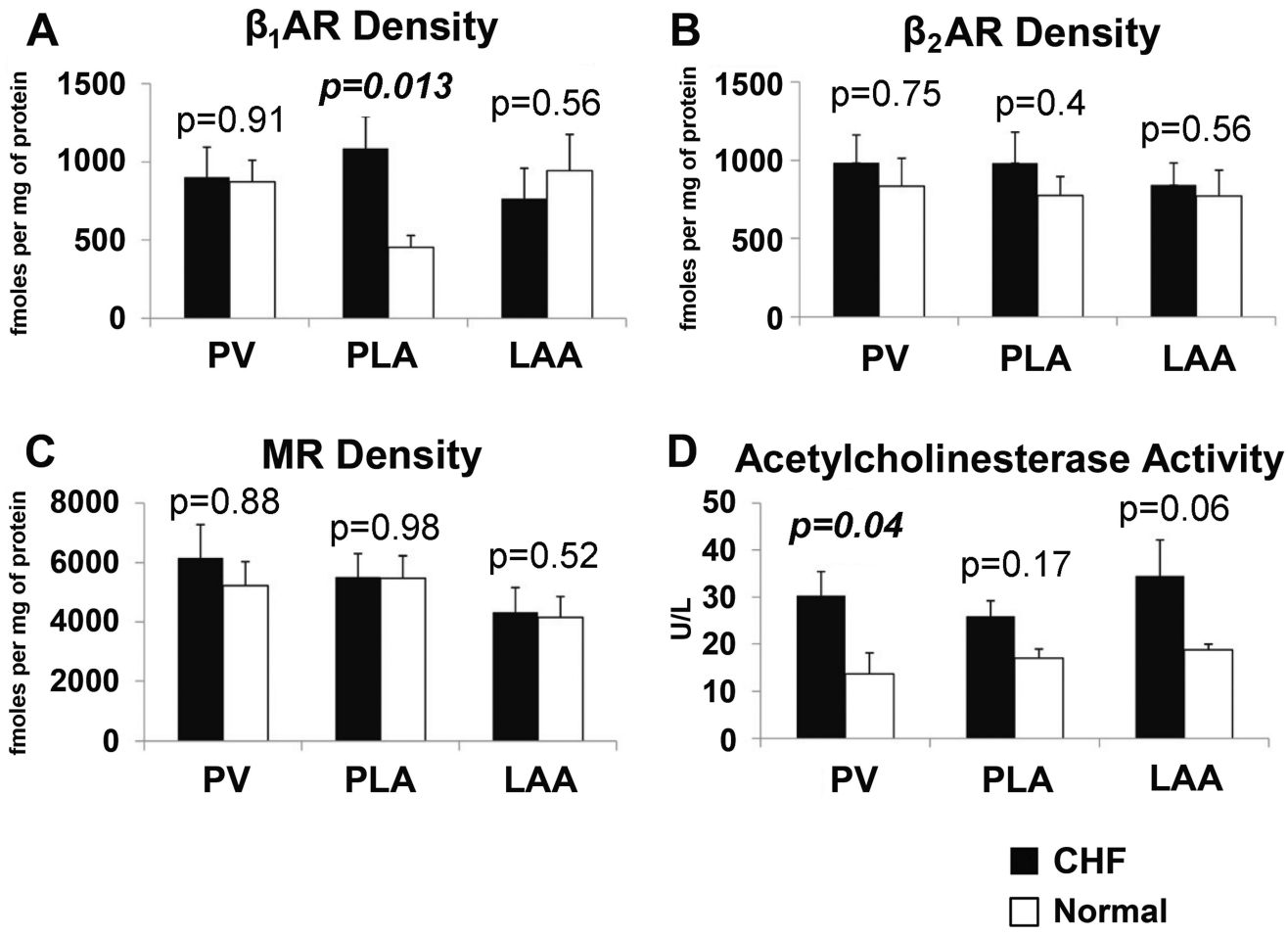

Figure 2.
Comparison of beta-adrenergic receptors (βAR), muscarinic receptors (MR), and acetylcholinesterase (AChE) in the PV, PLA and LAA for CHF and normal dogs.

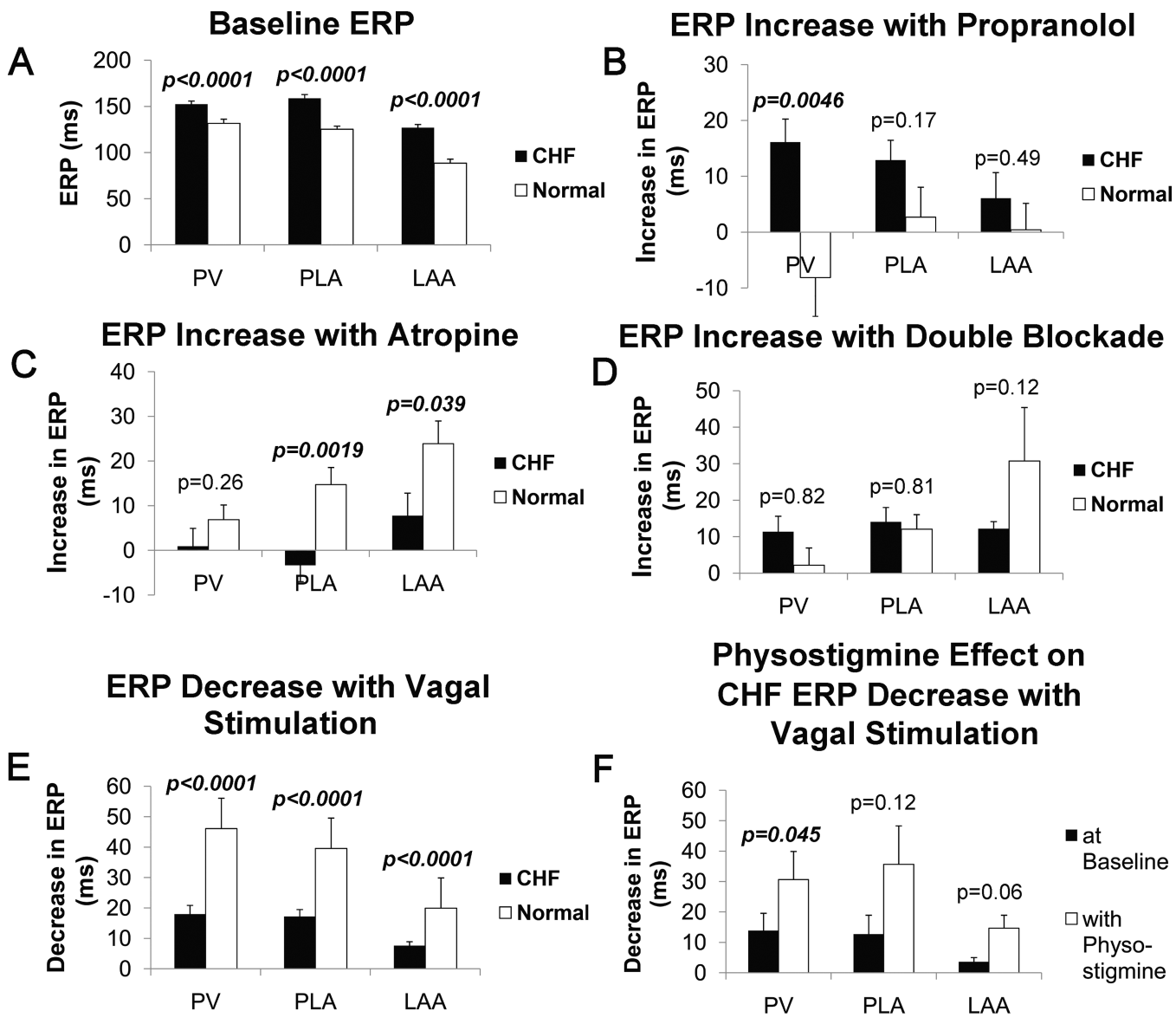

Figure 3.

Result of ERP testing obtained from the PVs, PLA, and LAA for CHF and normal dogs. A - ERPs at baseline; B – increase in ERP with propranolol; C – increase in ERP with atropine; D – increase in ERP with double blockade (combined propranolol and atropine); E – decrease in ERP with vagal stimulation effect; F – decrease in ERP with vagal stimulation effect for CHF dogs with and without physostigmine.

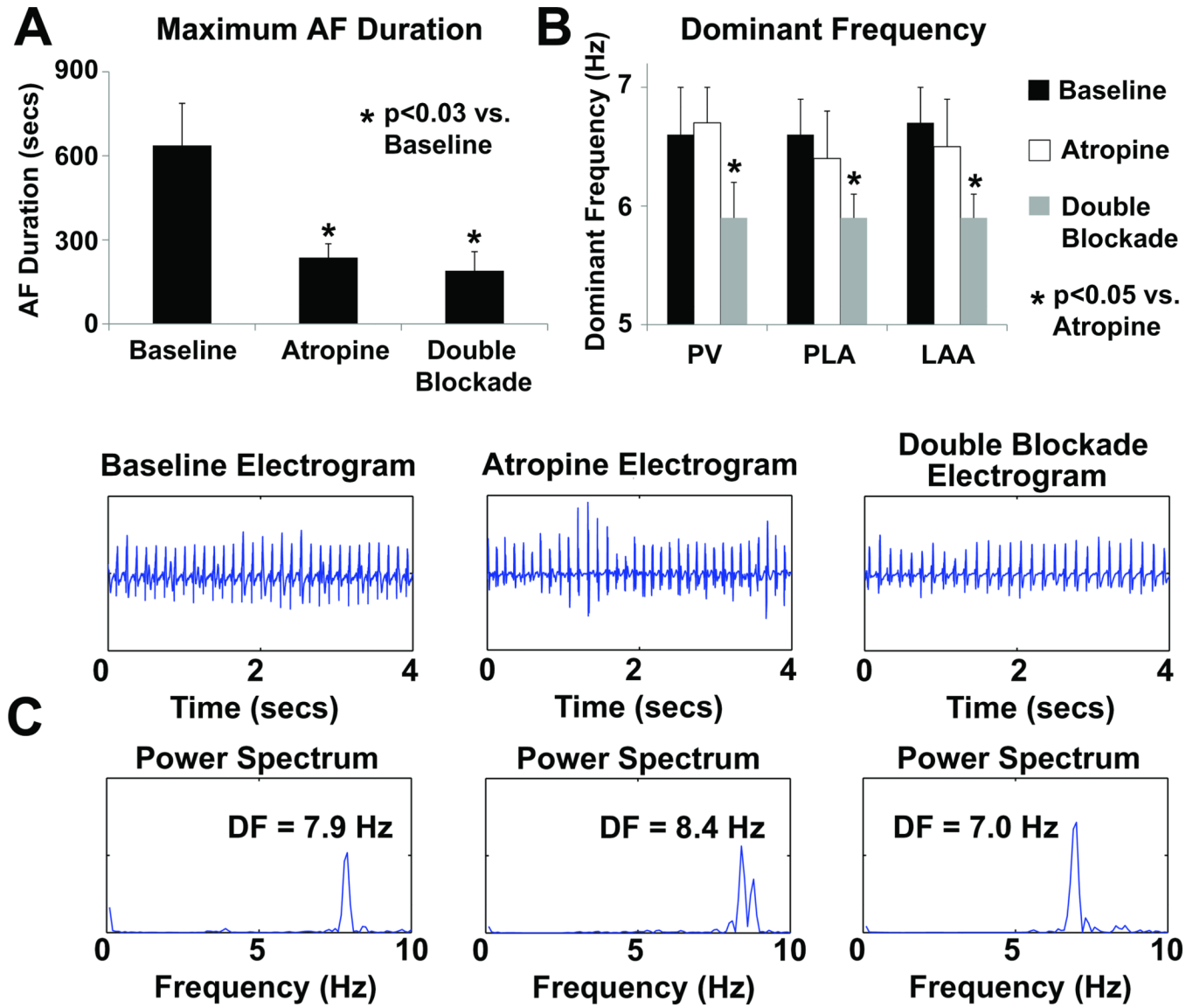

Figure 4.

Results of AF analysis in CHF dogs. A – Maximum AF durations obtained by burst pacing at baseline, with atropine, and with double blockade, B – Average dominant frequencies (DF) in the PVs, PLA and LAA at baseline, with atropine, and with double blockade. C – examples of PLA electrograms and corresponding power spectrum during baseline, with atropine, and with double blockade.

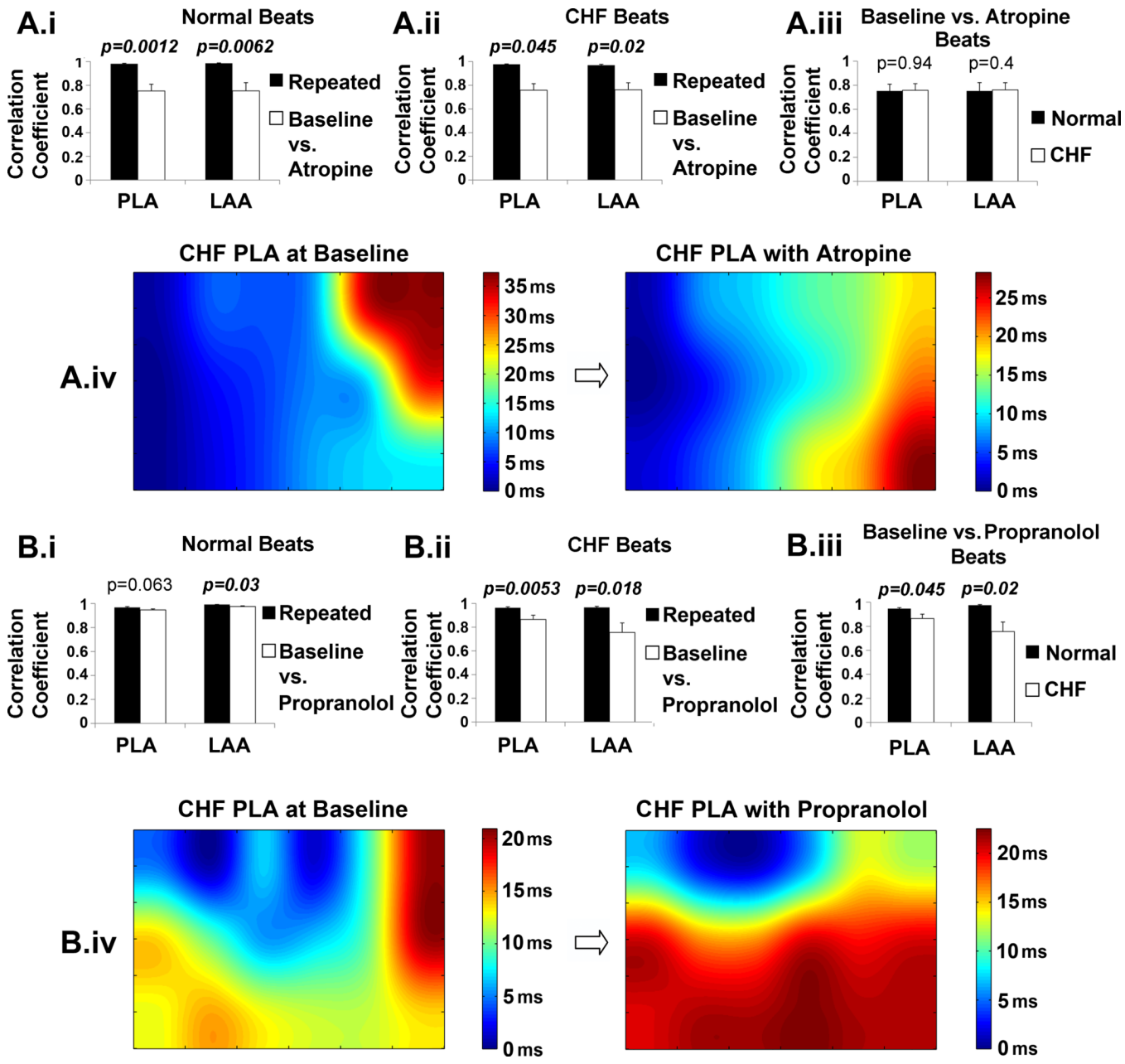

Figure 5.

Effect of autonomic blockade on activation patterns in the PLA and LAA for CHF and normal dogs. The corresponding results for atropine and propranolol are shown in panels A and B, respectively. A.i and B.i show the effect of autonomic blockade on conduction in the normal dog by comparing correlation coefficients of activation times from the repeated beats compared with the correlation coefficients obtained between baseline vs. autonomic blockade beats, A.ii and B.ii show the effect of autonomic blockade on conduction in the CHF dogs. A.iii and B.iii compare the correlation coeffients of activation times of the normal dogs vs. the CHF dogs. A.iv and B.iv show examples of activation maps from the PLA before and after autonomic blockade in a CHF dog.

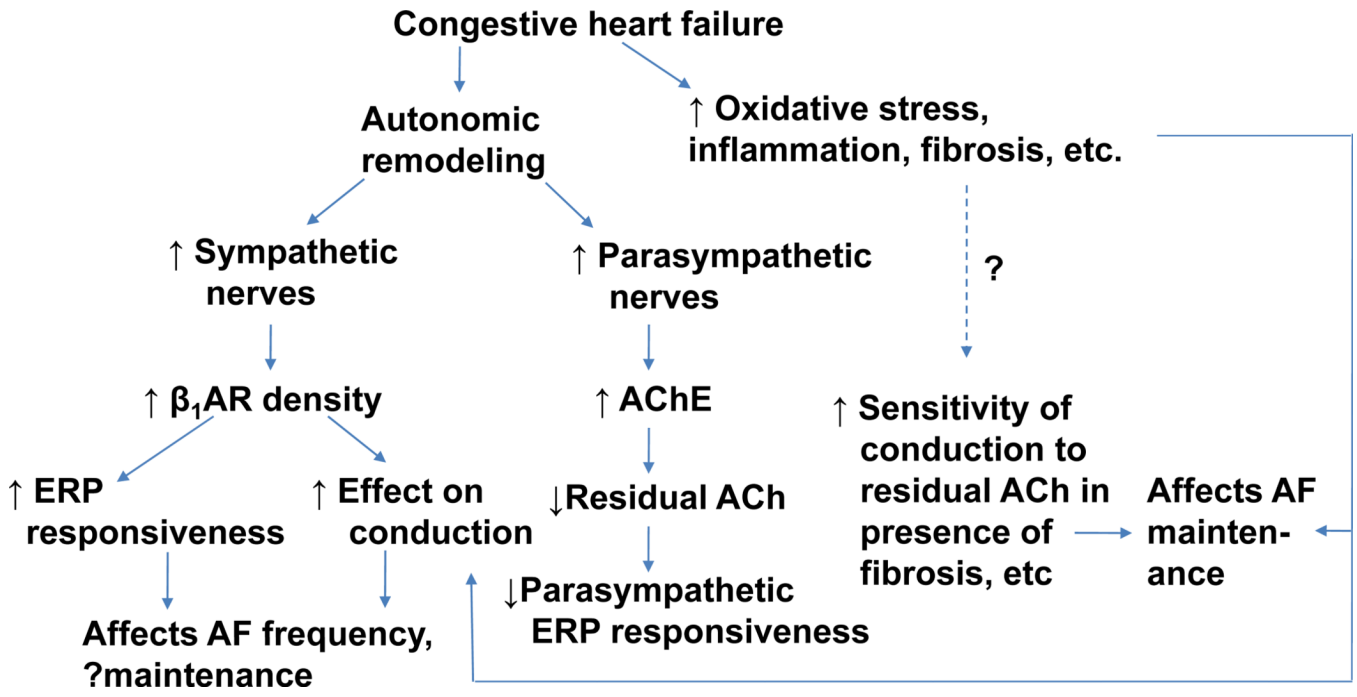

Figure 6.

Proposed model of creation of autonomic substrate for AF in CHF. The model suggests the likely presence of synergistic interactions between structural changes (fibrosis) and autonomic remodeling in the creation of AF substrate in heart failure.

ACh = acetylcholine, AChE = acetylcholinesterase, β_1AR – beta-1 adrenergic receptor, ERP = effective refractory period

Table 1

Sample sizes for analyses performed in this study.

Analysis	Intervention	N (CHF)	N (Normal)
Effective refractory periods	Cervical Vagal Stimulation	38	39
	Physostigmine	8	3
	Physostigmine + Vagal Stimulation	8	3
	Carbachol (1mmol/L)	8	7
	Atropine	16	17
	Isoproterenol	17	5
	Propranolol	18	15
	Propranolol + atropine	21	8
Atrial fibrillation Testing	Atropine	12	
	Atropine+propranolol	8	
Activation Mapping	Atropine	9	16
	Propranolol	15	10
Immunohistochemistry		11	7
β-adrenergic and muscarinic acetylcholine receptor densities		16	14
AChE activity		13	5
CCh dose response		59 cells from 3 dogs	29 cells from 3 dogs